SYSTEMATIC FREQUENCY SHIFTS AND QUANTUM PROJECTION NOISE IN NIST-F1*

S.R. JEFFERTS, T.P. HEAVNER, J. SHIRLEY, T.E. PARKER

NIST – Time and Frequency Division, 325 Broadway, BoulderCo 80305-3328 USA

E-mail: jefferts@boulder.nist.gov

We present results from NIST-F1, the NIST primary frequency standard, a Cesium atomic fountain. In particular we give the results of the latest frequency evaluation which has a combined standard fractional frequency uncertainty of 1.3×10^{-15} in the laboratory and a total uncertainty of 1.5×10^{-15} including the time transfer to the Bureau International des Poids et Mesures (BIPM) international atomic time scale (TAI). We also present results that demonstrate the attainment of the quantum projection noise limit in this fountain.

1 Introduction

NIST-F1 is a cesium-fountain primary frequency standard. The standard uses the (0,0,1) launch geometry of the seminal Laboratoire Primaire du Temps et des Frequences (LPTF) fountain [1], but differs in many significant ways from the LPTF standard. NIST-F1 has been reporting primary frequency standard numbers regularly since December 1999, and the latest frequency evaluation has the lowest combined standard uncertainty of any number hithertofore reported to the BIPM for inclusion into TAI.

2 Frequency Evaluation

Before a frequency measurement made with a primary frequency standard is included into TAI, it must be corrected for a number of significant (relative to the claimed accuracy) frequency shifts. Additionally a large number of other shifts must be evaluated to ascertain the relative importance of each. The frequency of NIST-F1 is typically corrected for shifts due to four causes: quadratic Zeeman effect, blackbody frequency shift, spin-exchange shift and the gravitational redshift [2].

The gravitational redshift is not properly a frequency shift intrinsic to the clock; however, TAI is computed with respect to the reference geoid (roughly mean sea level), and NIST-F1 is located some 1700 meters above mean sea level. The gravitational redshift at the location of NIST-F1 has been calculated by Weiss and

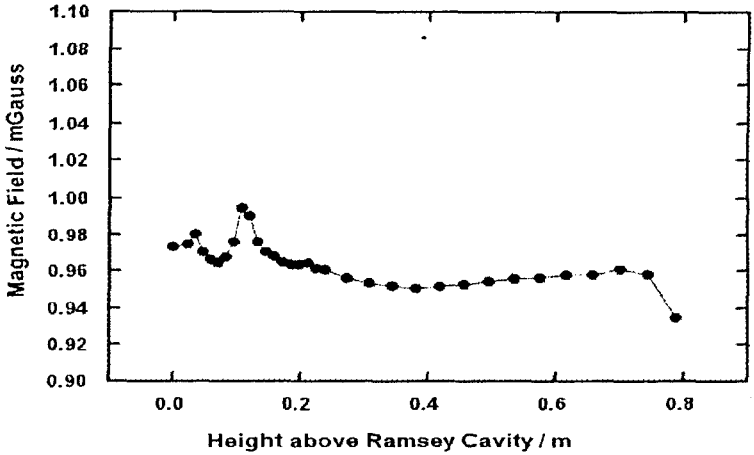

Figure 1 The measured magnetic field in NIST-F1 as a function of height above the Ramsey cavity. The origin of the x-axis is the center of the Ramsey cavity. The magnetic inhomogeneity just above the Ramsey cavity is a result of imperfectly adjusted shim coils that help to compensate for the magnetically permeable microwave feedthroughs on the Ramsey cavity.

Ashby to have a fractional frequency value of 180.5×10^{-15} with an uncertainty of 0.1×10^{-15} at the location of NIST-F1[3].

The quadratic Zeeman shift is a result of the purposely applied quantization magnetic field (C-field). A large advantage to the long interaction time available in atomic fountains is the consequent ability to reduce the magnitude of the C-field. The typical C-Field value in NIST-F1 is of order 100 nT (10^{-3} gauss), much smaller than the typical 5 μT field used in a thermal beam standard. The resulting frequency correction is thus more than three orders of magnitude smaller.

The correction for the quadratic Zeeman frequency shift requires knowledge of the time averaged magnetic field as seen by the atoms. We obtain this information from a map of the magnetic field as seen by the atoms as shown in Fig1. The magnetic field map is measured using the linear Zeeman splitting of the $m\neq1$ levels as discussed in [2]. Basically the atoms are irradiated with a low frequency magnetic field transverse to the quantization axis for a short (≈100 ms) period about apogee. If the transverse field is resonant with the $\Delta F=0$, $\Delta m=1$ transition frequency the resulting change in atomic state is detected, which, in turn, gives a measure of the local magnetic field. The apogee height is then changed and the process is repeated in order to generate the field map. Using the field map the time averaged magnetic field as seen by the atoms can be calculated. This average should correspond to a particular Ramsey fringe on the magnetically sensitive Ramsey fringe manifolds at all apogee heights. Figure 2 shows a comparison of

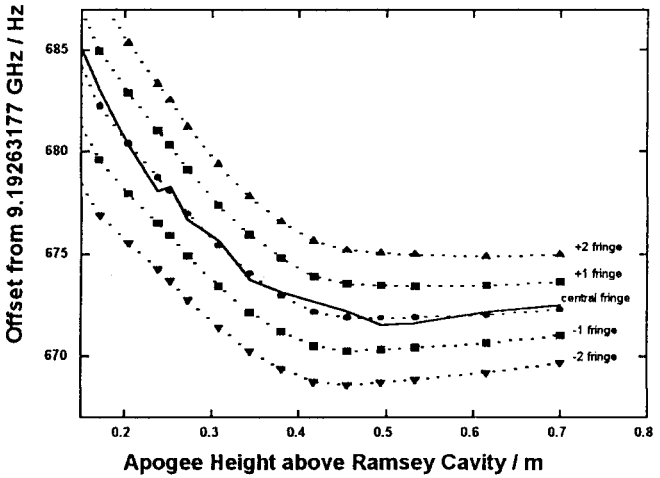

Figure 2 - The various symbols connected by dotted lines are the measured position of Ramsey fringes on the $|3,1\rangle \rightarrow |4,1\rangle$ manifold. The solid line is a prediction of the position of the central fringe from an integral of the time average magnetic field seen by the atom using the data of Fig. 1.

the measured vs. calculated fringe position; the comparison has an average discrepancy of 0.05±0.2 fringes, indicating that the central fringe on the m=+1 Ramsey manifold is correctly identified. Using the measured offset (from the m=0 central fringe) frequency, ν_{10}, of the m=1 central Ramsey fringe the fractional frequency correction, $\Delta\nu_{QZ}/\nu_o$, to the measured fountain frequency, ν_o, is given by

$$\frac{\Delta\nu_{QZ}}{\nu_o} = \frac{8\nu_{10}^2}{\nu_0^2}.$$

In the case of NIST-F1, the fractional frequency correction is of order 45×10^{-15} with an assigned uncertainty of 0.3×10^{-15}, which corresponds to a mis-assignment of one complete fringe.

The next largest shift for which the fountain frequency is corrected is the blackbody shift, first predicted by Itano et. al. [4]; the coefficients required to make this correction have been recently measured by both the LPTF and PTB groups [5,6]. The correction is given by

$$\frac{\delta\nu}{\nu_o} = -1.711(3)\times10^{-14}\left(\frac{T}{300K}\right)^4 \times \left[1 + 0.014\left(\frac{T}{300K}\right)^2\right],$$

where T is the temperature of the radiation field in which the atoms are situated. The temperature of NIST-F1 is controlled to 41 °C. In and above the Ramsey cavity, the atom is surrounded by the copper vacuum envelope. The window at the top of the vacuum envelope through which one of the vertical laser beams enters is anti-reflection coated at 852 nm, and is quite black at wavelengths longer than 3μm. These considerations lead us to a conclusion that the radiation field experienced by the atoms should be a close approximation to the temperature of the vacuum wall. We assign a possible 1 °C discrepancy to the radiation temperature, which leads to an uncertainty in the fractional frequency correction of 0.3×10^{-16}.

The last frequency shift for which NIST-F1 is corrected, the spin-exchange frequency shift, while the smallest in absolute magnitude dominates the systematic part of the error budget. The spin-exchange frequency shift in cesium has been recognized as a significant problem since the earliest days of cesium fountains [7]. Both Gibble and Chu at Stanford and later the group of Clairon at the LPTF have measured large spin-exchange frequency shifts in cesium atomic fountains [8]. Since these measurements were made it has been recognized that the spin-exchange coefficient is not only large, but is probably not constant in the collision energy ranges typically accessed by cesium fountains [9].

The spin-exchange frequency shift is, all other things being equal, linear in the atomic density. Typically, the frequency correction to be applied for the spin-exchange shift is measured via an extrapolation of the measured frequency vs. atom number curve measured under otherwise constant parameters. Such a curve, from NIST-F1, is shown in Fig.3. The intercept (at zero atomic density) of the extrapolated line with the frequency axis therefore gives the "true" frequency in the absence of the spin-exchange shift.

In a freely expanding non-interacting gas of atoms, the collision energy drops with the time since the expansion started with a time constant τ such that $\tau\propto R_{cloud}/V_{rms}$ where R_{cloud} is the characteristic dimension of the cloud (the radius if the cloud is spherical) and V_{rms} the characteristic velocity of the atoms in the cloud with respect to the center-of-mass velocity, $V_{rms}\propto(kT/m)^{1/2}$ for a thermal distribution. Given that the radius of a sample of atoms trapped in an MOT is dependent on the number of trapped atoms, the historical practice of using a MOT to gather atoms and varying the loading time in order to vary the atom number to generate a curve such as Fig. 3 is perhaps improper given the present understanding that the spin-exchange coefficient is collision energy dependent. NIST-F1 uses a pure optical molasses source that gives an unvarying cloud shape over more than the range of atomic densities used to obtain the data in Fig. 3. The data in Fig. 3 were gathered using an active atom number stabilization servo. The servo changes the power in the state-selection cavity to bring either more or fewer atoms into the selected $|3,0\rangle$ clock state and can be used with an MOT operated in

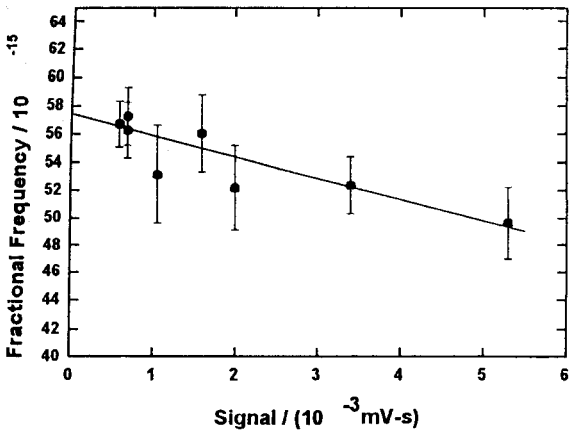

Figure 3 – Spin-exchange frequency shift data: measured fractional frequency of the maser as corrected to the NIST AT1E time scale as a function of detected atom number. The intercept of the curve is the zero density limit of the measurements.

the condition of constant atom number to keep the collision energy constant. This approach has been recently adopted for the PTB fountain [10].

The data in Fig. 3. were used to generate the line shown. The uncertainty in the intercept of the frequency axis is $\delta f/f = 1.2\times10^{-15}$ which we regard as a combination of statistical (Type A) uncertainty and systematic (Type B) uncertainty. If there were no spin-exchange shift we would be free to group the data in Fig. 3. into a single measurement of frequency, and the error bars on the resulting point would be the combined statistical error in the various measurements, in this case $\delta f/f = 0.8\times10^{-15}$. The rms difference between the combined uncertainty (the uncertainty in the intercept) and the statistical uncertainty is then the systematic uncertainty associated with the spin-exchange shift, $\delta f/f = 0.9\times10^{-15}$.

Numerous other possible biases exist that are discussed, for NIST-F1, in [2].

The combined (Type B) uncertainty of the four significant systematic frequency shifts in NIST-F1, gravitational redshift, blackbody shift, quadratic Zeeman effect and the spin exchange shift are $\delta f/f = 1\times10^{-15}$ with a statistical uncertainty of $\delta f/f = 0.8\times10^{-15}$, these combine to give a total combined standard uncertainty of $\delta f/f = 1.3\times10^{-15}$ in the laboratory. The evaluation discussed here lasted 40 days, starting from MJD 52079, and the corrections for dead time are small with respect to the combined standard uncertainty. However, the frequency-transfer noise associated with the GPS common-view time-transfer used to report the clocks to the BIPM for inclusion into TAI is $\delta f/f = 30\times10^{-15}/\tau$ where τ is in

days. This results in a significant degradation in the accuracy of the reported number, to $\delta f/f = 1.5\times10^{-15}$, when included into TAI. Had the period of the evaluation been a more normal 20 days instead of 40 days, the number would have degraded to 2×10^{-15}. Clearly, fountains are becoming sufficiently accurate that the strain on the time-transfer reporting method is noticeable.

3 Quantum Projection Noise

Quantum projection noise, first described by Itano et. al. [11] has been observed previously, first in ions [11] and later in atomic cesium fountains [12]. We report our first observation of quantum projection noise bringing to two the number of observations of this behavior in fountains.

The stability of a cesium fountain clock can be written as [12]

$$\sigma_y(\tau) = \frac{1}{\pi Q_{at}}\sqrt{\frac{T_c}{\tau}}\left(\frac{1}{N_{at}} + \frac{1}{n_{ph}N_{at}} + \frac{2\sigma_{\delta N}}{N_{at}^2} + \gamma\right)^{1/2},$$

where Q_{at} is the atomic line Q, T_c is the cycle time, N_{at} is the number of detected atoms, n_{ph} is the number of detected photons/detected-atom, $\sigma_{\delta N}$ represents the technical noise in the detection process in terms of an equivalent number of atoms, and γ is the noise associated with the local oscillator and aliasing effects. The first term in the brackets is the quantum projection noise term, the second term which

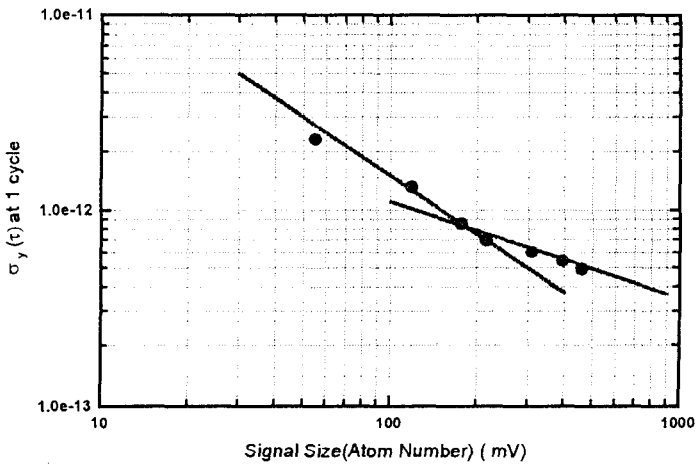

Figure 4 - Allan variance vs. atomic number. The straight lines have slopes of -1 and -1/2 respectively to illustrate the behavior in the technical noise limited regime as well as the quantum projection noise regime

scales in the same way with atom number is much smaller in NIST-F1, where the number of detected photons, n_{ph}, is large (n_{ph}>>10). The third term dominates at very low atom numbers while the forth term, associated with the quartz local oscillator is small relative to the first three terms in the experiment described here.

The data in Fig. 4 show the Allan variance at τ = 1 cycle vs. detected signal which is proportional to the number of detected atoms. These data were gathered using the same technique used in our active number servo: the atom number was varied for these tests by varying the power in the state-selection cavity with all other parameters held constant. The Allan variance for signal sizes less than about 200 mV has the $1/N_{at}$ behavior associated with technical noise while the data at signal sizes larger than 200 mV have a slope consistent with $(1/N_{at})^{1/2}$, which represents quantum projection noise. This data while certainly suggestive that the quantum projection noise limit has been achieved is not, in itself, sufficient to unambiguously support the claim.

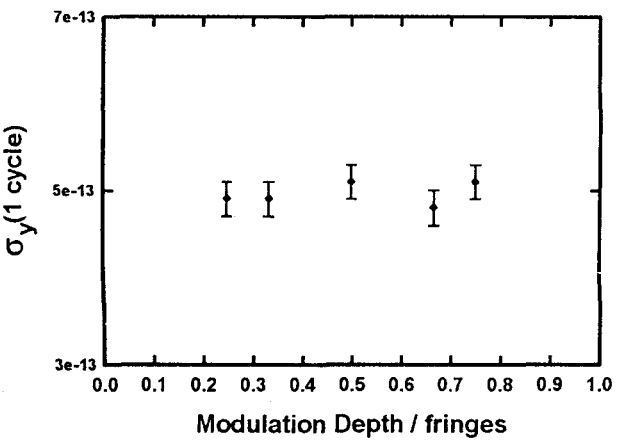

Figure 5 - The Allan variance of the fountain is constant over a large variation in modulation depth in the quantum projection noise limited regime.

Another signature that the projection noise limit has, in fact, been reached can be obtained by measuring the stability of the standard in the quantum projection noise limit with non-optimum modulation. If the noise is, in fact, set by the atomic number the non-optimum modulation depth should not cause an increase in noise. Otherwise the noise should increase with non-optimum modulation. The data shown in Fig. 5, taken at relatively high atom number, clearly shows that the noise is independent of modulation depth over almost a factor of 4 in modulation width.

The data in Fig. 4 can be evaluated to show that NIST-F1 reaches the quantum projection noise limit at about 2500 detected atoms with an equivalent noise, $\sigma_{\delta N} \approx 35$ atoms.

4. Conclusions

The first results from a cesium atomic fountain operating as a primary frequency standard were presented at the last meeting of this conference [1] in Woods Hole in 1995. In the past 6 years the field has matured dramatically with many laboratories working on cesium fountain primary frequency standards and two standards, from the PTB and NIST, regularly reporting numbers to the BIPM. We have discussed here our frequency uncertainty evaluation procedure, the PTB evaluation procedure is discussed in these proceedings as well. Both of the regularly reporting standards (PTB and NIST) have combined standard uncertainties in their respective laboratories below $\delta f/f < 1.5 \times 10^{-15}$. In addition these standards have been compared using advanced time-transfer techniques over the past year and the agreement is good within the stated uncertainties [13]. It will be interesting to see what the state of the art is at the 7th Symposium on Frequency Standards and Metrology.

References

1. Clairon A., et. al., in *Proc. 5th International Symposium of Frequency Standards and Metrology*, World Scientific(1996) pp49-59.
2. Jefferts, S.R. et. al., submitted to *Metrologia*.
3. Weiss, M.A., Ashby, N., *Metrologia.* **37** (2000) pp. 715-17.
4. Itano, W.D., Lewis, L., Wineland, D., *Phys.Rev. A.*. **45** (1982) pp. 1233–35.
5. Bauch, A., Schroeder, R., *Phys. Rev. Lett,* **78** (1997) pp. 622-25.
6. Simon, E., Laurent, P., Clairon, A., *Phys. Rev. A.,* **57** (1998) pp. 436–39.
7. Gibble, K., Chu., S., *Phys. Rev. Lett.* **70** (1993) pp. 1771–74.
8. Ghezali, S., et. al.. *Europhysics Lett.*, **36** (1996) pp. 25–30.
9. Leo, P.J., et. al., *Phys.Rev.Lett.*, **86**(2001)pp.3743-46.
10. Weyers, S., et. al., *These Proceedings.*
11. Itano, W.D., et. al., *Phys. Rev. A* **47** (1993) pp.3554-70.
12. Santarelli, G., et. al., *Phys. Rev. Lett.* **82** (1999) pp. 4619-22.
13. Parker, T.E., *These Proceedings*